

Efficiency of Self-Healing Microcapsules in Concrete Slabs Subjected to Low Velocity Impact Force

Salima Al Badi¹, Zarina Itam^{2*}, Wong Leong Sing², Muhammad Imran Najeeb³, Nazirul Mubin Zahari², Afeeq Haiqal Mohd Hafiez⁴, Shaikh Muhammad Mubin Shaik Ahmad Fadzil², Mohd Meer Saddiq Mohd Sabee⁵ and Zuratul Ain Abdul Hamid⁵

¹*College of Graduate School, Universiti Tenaga Nasional, Jalan IKRAM-UNITEN, 43000 Kajang, Selangor, Malaysia*

²*Institute of Energy Infrastructure, Universiti Tenaga Nasional, Jalan IKRAM - UNITEN, 43000 Kajang, Selangor, Malaysia*

³*Department of Engineering Education, Faculty of Engineering and Built Environment, Universiti Kebangsaan Malaysia, 43600 Bangi, Selangor, Malaysia*

⁴*Department of Civil Engineering, Universiti Tenaga Nasional, Jalan IKRAM - UNITEN, 43000 Kajang, Selangor, Malaysia*

⁵*Biomaterials Research Niche Group, School of Materials and Mineral Resources Engineering, Universiti Sains Malaysia, 14300 Nibong Tebal, Pulau Pinang, Malaysia*

ABSTRACT

Plentiful modern buildings in urban and rural zones, especially buildings constructed from reinforced concrete (RC) materials, were exposed to severe defects such as spalling and delamination as the years progressed. The most used method to repair damages on existing RC is through the use of shotcrete cement grout or heavy-duty structure tape retrofits. These methods involved multiple manpower, modern equipment and a longer time of structural healing, which led to a higher cost of

maintenance. Therefore, the application of self-healing microcapsules within the RC structures is one of the solutions to support the rehabilitation of cementitious-based products by developing a building with self-healing properties. This research investigates the concrete's self-healing performances subjected to low velocity impact using large (L) and small (S) self-healing microcapsules measured at 70 mm × 10 mm and 70 mm × 5 mm. The positions (Point 1, 2 and 3) of the microcapsule in the concrete were placed based on the simulated results of severe cracks on the impacted control concrete sample from the ANSYS explicit dynamics. Post impact results

ARTICLE INFO

Article history:

Received: 23 May 2024

Accepted: 24 December 2024

Published: 11 June 2025

DOI: <https://doi.org/10.47836/pjst.33.4.01>

E-mail addresses:

Salimaroyalpalac2023@gmail.com (Salima Al Badi)

imran.najeeb@ukm.edu.my (Muhammad Imran Najeeb)

izarina@uniten.edu.my (Zarina Itam)

WongLS@uniten.edu.my (Wong Leong Sing)

Nazirul@uniten.edu.my (Nazirul Mubin Zahari)

afeeq.nikon@gmail.com (Afeeq Haiqal Mohd Hafiez)

smmubin27@gmail.com (Shaikh Muhammad Mubin Shaik

Ahmad Fadzil)

meersaddiq@gmail.com (Mohd Meer Saddiq Mohd Sabee)

srzuratulain@usm.my (Zuratul Ain Abdul Hamid)

* Corresponding author

show that the concrete with L microcapsules had 68.2% more self-healing efficiency compared to S microcapsules, showing it had better damage recovery.

Keywords: Crack reduction, drop weight test, energy efficiency, reinforced concrete slabs, self-healing microcapsules

INTRODUCTION

Reinforced concrete (RC) has become one of the most broadly applied components in construction, in addition to steel structures. RC is proven as a very strong structural element for an infrastructure's column, beam, wall, and slab, but it deteriorates as the years progress. This, in return, degrades the materials bonded within the building (Lv et al., 2022). Generally, concrete has low tensile strength and durability, but the implementation of steel reinforcement bars boosts the toughness of the concrete. The steel reinforcement bars are protected from the damage caused by the alkaline environment formed in the RC, yet due to defects in the structure that are prone to breaking down from outside mechanical stress, it forms problems such as drying or self-shrinking (Muhammad et al., 2016). Thus, through the fissures, the reinforcement becomes exposed to acidic ions, which causes it to corrode and ultimately weaken the concrete. In an attempt to improve the mechanical properties of RC, concrete mix design or proportions went through plenty of changes in terms of material choices throughout the years (Muhammad et al., 2016).

Numerous researchers are currently conducting a comprehensive study on the moderated environmental impact of RC, especially studies on repairing and rehabilitating RC structures from early production (Hilloulin et al., 2015). The studies are an initiative to reduce the repair and maintenance costs of the structures. Recently, the frequently used method to repair damage on existing RC is through shotcrete cement grout or heavy-duty structure tape retrofits (Vijay et al., 2017). The actions to repair the RC with these methods will involve multiple man-hours, modern equipment, and a longer time for structural healing, which leads to a higher cost of maintenance. The application of self-healing microcapsules within the RC structures is one of the latest types of research to support the rehabilitation of cementitious-based products by developing a building with self-healing properties (Mir et al., 2023). Concrete is susceptible to cracking due to various factors such as shrinkage, temperature changes, and external loads. Normal concrete is brittle, causing it to fail without warning. The traditional repair methods for concrete structures are costly and labour-intensive. However, the reports show that concrete repairs are performed inconsistently and failure rates are high, and it was estimated that nearly half of the traditional concrete repairs fail in the field. Additionally, the replacement and repair activity with new concrete often has a substantial environmental impact due to the production and disposal of waste materials (Yıldırım et al., 2018). Self-healing microcapsules release healing agents that can fill these cracks, effectively repairing the

damage and restoring the concrete's strength and durability. Therefore, a self-healing system that treats internal defects without human intervention is one of the most desired properties in material science and engineering.

Concrete is one of the most widely used construction materials globally, but its production has a considerable environmental impact due to the extraction of raw materials and high energy consumption. By enhancing the durability of concrete structures, self-healing technology reduces the need for new concrete production and promotes a more sustainable approach to construction. The self-healing microcapsules' utilisation in RC slabs supports several UNESCO Sustainable Development Goals (SDGs). SDG 9 promotes resilient infrastructure, inclusive industrialization, and innovation. Using self-healing microcapsules in concrete falls under innovation in construction materials and techniques. These microcapsules contain healing agents released when cracks form in the concrete, effectively repairing the damage independently. This innovation can enhance the durability and lifespan of concrete structures, reducing the need for frequent repairs or replacements, and ultimately promoting more sustainable infrastructure development.

Additionally, self-healing concrete contributes to the United Nations initiative in the SDGs by improving the sustainability and resilience of infrastructure. This aligns with SDG 9, which promotes resilient infrastructure through innovative materials. Besides that, self-healing concrete improves the longevity and durability of the structure, minimising the waste of material due to frequent replacements/damages. These attributes align with and support SDG 11 (sustainable cities and communities) and SDG 12 (responsible consumption and production).

By automatically repairing cracks as they occur, self-healing concrete can extend the lifespan of structures. This reduces the need for frequent repairs or replacements, saving time, money, and resources in the long run. Cracks in concrete can lead to water infiltration, which can cause corrosion of the embedded reinforcement, compromising the structure's overall safety. Self-healing concrete minimises the potential for further damage and ensures the safety of the infrastructure. Hence, the capability of self-healing capsules to repair concrete initial and severe cracks is anticipated as a further environmentally friendly building practice (Van Tittelboom et al., 2011).

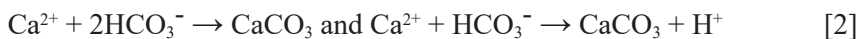
Previous research by Zhang et al. (2020) discovered that concrete's capacity for self-healing is an autogenous process where numerous chemicals and materials were experimented with in order to identify the optimum potentials and efficiency in self-healing agents (Zhang et al., 2020). Variation of healing agents that consisted of sodium silicate, polyurethane, epoxy, cyanoacrylates, and bacterial spores has been studied to effectively rehabilitate RC components (Zhang et al., 2020). However, fewer articles in engineering describe the efficiency and validations of using the various healing agents to reduce the width of the cracks on the RC surfaces. The authors formed three types of self-healing processes: natural self-healing, chemical self-healing, and biological self-healing processes

(Althoey et al., 2023; Zhang et al., 2020). The natural self-healing process is a process that partially heals cracks in RC naturally with the formation of CaCO_3 or CaOH from the self-healing agents, such as calcium nitrate and sodium silicate (Althoey et al., 2023). The agents react with the impurities during water transport as well as the hydration of unreacted ordinary Portland cement. Hydrated cement patterns like calcium silicate hydrate gel are then formed at the crack zones, which will repair the cracks on the RC surfaces (Jogi & Lakshmi, 2021).

The creation of calcium carbonate and calcium hydroxide is among the important factors for the natural repair of concrete. The initial phase of the healing process by the self-healing agent is carbon dioxide, which dissolves in water as shown in Equation 1 (Rosewitz et al., 2021).



Then, a reaction occurred between pH7.5 to pH8 in the cement, which led to the development of calcium carbonate crystals after the loss of calcium ions into the RC as a system of cement hydration, as shown in Equation 2 (Rosewitz et al., 2021).



Universally, the chemical process of self-healing is known as a chemical healing technique that is supported by chemical compounds. Self-healing RC is made through the injection of liquid chemical reagents into small containers of fresh RC structure (Restuccia et al., 2017). The chemical self-healing process is performed through the passive method, where the chemicals are stored in a capsule or other materials of hollow shapes and applied into the structure during the construction process. The liquid within the capsules is transferred throughout the fractures and repaired the cracks in due course (Restuccia et al., 2017). Furthermore, a detailed study that was accomplished proved the capsules fractured after bending test released adhesive at 20% of its weight (Jakubovskis et al., 2020). According to Homma et al. (2009), specimens of self-healing RC can recover 26% of the RC's initial strength compared to restrained specimens that recovered by 10%. Thus, the increase in the quantity of self-healing agents inside the capsules increased the strength of the repair rate of the RC structures.

From the perspective of the biological self-healing process, the use of microorganisms in RC is considered a biological application for self-healing, as the microorganism can cover the crack in any condition, including cold or warm, water and soil (Jakubovskis et al., 2020). The researcher of self-healing properties mentioned that polymorphic ferro-aluminium silicate and calcium carbonate are necessary for precipitation to produce a self-healing reaction on RC structures. The microbial broth of the microorganisms is alternatively encapsulated inside microbial encapsulation before implementation into the

fresh RC mix to improve the condition of structures. Strong self-healing by employing a microencapsulation approach depends on how the healing agent works alongside the concrete to create healing after cracks occur.

The autogenous process of self-healing is influenced by the increment degree of hydration of the concrete and the calcium hydroxide carbonisation (Gupta et al., 2017). The solution of sodium silicate is one of the self-healing agents that produces carbonisation through RC hydration to heal the cracks over time and is preferred due to its hydration-enhancing characteristics, ready availability, and low cost in the engineering industry. The self-healing agents are labelled as monomer liquid in a plastic-based material, microcapsules. The microcapsules are capable of microcracking, which can lead to the liquid to release in an instant if a crack occurs within the structures (Durga et al., 2021). The model of microcapsules is created from pure polymers and a polymer layer which has a tensile strength of 0.73MPa to 1.2MPa, respectively (Khaliq & Ehsan, 2016). The literature indicates that self-healing microcapsules are engineered to release healing agents via various triggers, including mechanical stress, temperature, light, pH changes, and ion interactions, as shown in Table 1 (Gao et al., 2022; Lv et al., 2020; Ren et al., 2021; Xiong et al., 2015). However, research on the low-velocity impact of concrete remains insufficiently explored. In real-world applications, concrete is also susceptible to impact damage, resulting in sudden failure, a critical concern distinct from flexural and compressive stress.

This research aims to determine the performance of 70 × 10 mm (large) and 70 × 5 mm (small) polymeric microcapsules filled with sodium silicate liquid to heal ultimate cracks in the concrete slab specimens subjected to a 200 mm height of low velocity impact. Furthermore, investigation of the efficiency rate of microcapsules in terms of the rehabilitation process or crack reduction analysis on the specimens was also conducted. The healing mechanism will determine current self-healing limitations such as reliance on environmental conditions, microcapsule dosage, and crack width. For these reasons,

Table 1
Summary of past work on the development of self-healing microcapsules

Trigger type	Mechanism of trigger	Description	Material of capsule/core
Physical	Mechanical fracture	Mechanism of rupture under stress (flexural and compressive)	sodium carbonate (Na ₂ CO ₃) and calcium acetate (Ca(CH ₃ COO) ₂)
	Temperature	At a certain temperature, the microcapsule activated	polymethylmethacrylate-methacrylate shell and magnesium oxide core
	Light	Activate when there is light exposure	Epoxy acrylate-based free radical-cationic UV curable adhesive, A331
Chemical	pH	Responsive to pH change	Acrylate-based microcapsules
	ion	Release inhibitors to prevent corrosion of steel in concrete	Ag-alginate capsules with oil cores

research into healing mechanisms is critical, as results of the study may allow for the optimisation of a self-healing method as well as the establishment of conditions for proper implementation in the future of RC maintenance (Dixit et al., 2021).

MATERIALS AND FABRICATION

The self-healing microcapsules’ efficiency in RC slab subjected to low velocity impact force was conducted according to the flowchart as presented in Figure 1. Prior to testing, the location of the self-healing microcapsule was determined using simulation software based on the results of severe crack formation on the impacted control RC. Two types of self-healing microcapsules (small and large) are prepared and embedded in three spots

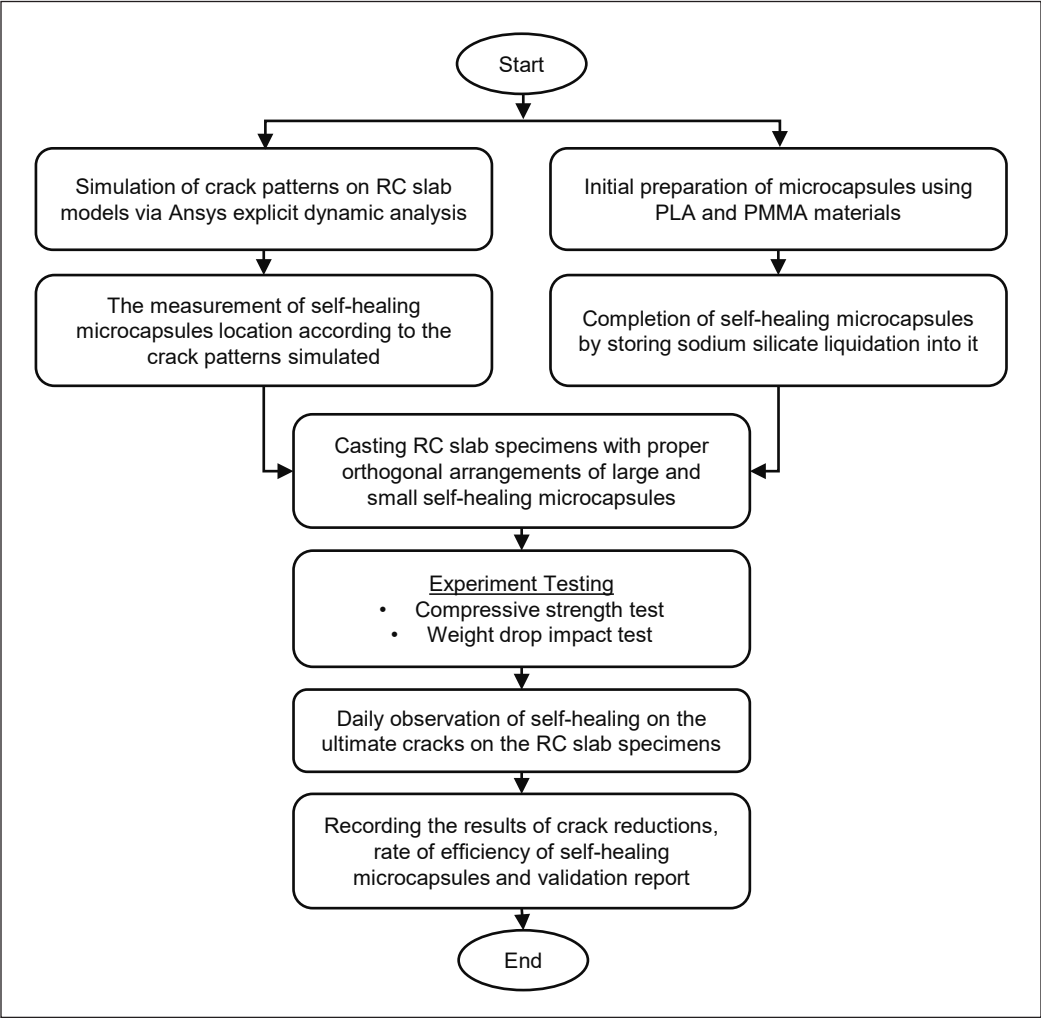


Figure 1. Flowchart of the research work

on RC slabs. Low-velocity impact tests were conducted on RC slabs with small and large self-healing microcapsules, with three repetitions for each type. The crack gap around the microcapsule was recorded and compared for both RC slabs for 28 days.

Types and Preparation of Self-Healing Microcapsules

The microcapsules were prepared from the use of polylactic acid (PLA) and polymethyl methacrylate (PMMA) materials that resemble transparent thermoplastic or acrylic glass components (Khaliq & Ehsan, 2016). A thermal printing machine moulded PLA and PMMA into a hollow cylinder. Then, the elongated hollow cylindrical shapes were cut into an equivalent length of 70 mm. The thickness between the inner and outer circles of the microcapsules is 2 mm. The microcapsules were moulded into two different diameters, which are 10 × 70 mm (large) and 5 × 70 mm (small), as shown in Figure 2.

The microcapsules were created to encapsulate the chemically pure (C.P.) sodium silicate liquid as a self-healing agent in order to repair the RC slab specimens internally after the occurrence of ultimate cracks (Khaliq & Ehsan, 2016; Durga et al., 2021). A strong waterproof silicone sealant sealed one end of the self-healing microcapsule. Sodium silicate liquidation was then injected into the self-healing microcapsules. The microcapsules were sealed again on the other end to secure the agent. The chosen self-healing material is because it has shown success in healing properties reported in several studies (Irico et al., 2017; Li & Guan, 2023; Mokhtar & Hassan, 2021). This method is particularly advantageous because it offers a good response to crack formation, enhances the durability and longevity of concrete structures, and requires minimal intervention once applied. To extend the work on this material, the author investigates the concrete healing performance with two different sizes of self-healing microcapsules subjected to low-velocity impact.

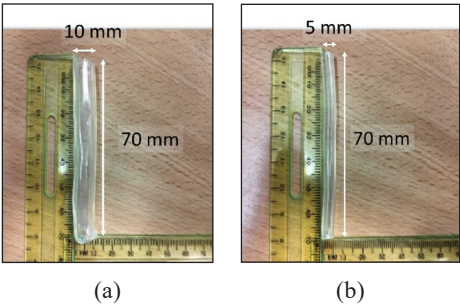


Figure 2. (a) Large self-healing microcapsules; and (b) Small self-healing microcapsules

Arrangement of Self-Healing Microcapsules

Following the preparations of the self-healing microcapsules, a numerical simulation for explicit dynamic analysis of the concrete slab specimen was performed via ANSYS analysis software. The material properties of the concrete slab and stainless-steel ball impactor used are as per Table 2 (Ferrara et al., 2018).

The concrete slab was developed with a size of 305 mm × 305 mm × 50 mm, with a steel ball for impact loading at a diameter of 110 mm. The boundary conditions of the concrete model were set as a four-sided fixed support. The explicit dynamic analysis was performed,

and the results demonstrated that the cracks were formed in a critical orthogonal crack pattern with crack initiation and orientation at the middle of each side of the slab. The critical zones of the cracks on the model were presented in Figure 3(a).

The crack patterns from the low-velocity impact result obtained from the numerical simulation were used to determine the number of self-healing microcapsules as well as the distance or location of each self-healing microcapsules within the concrete slab specimens. The length of 305 mm was divided into two (152.5 mm) to identify the centre of the slab specimens as seen in Figure 3(b). Ten self-healing microcapsules, either large or small in size, were then placed in the slab specimens, where the distance

Table 2
Material properties form explicit dynamic analysis

Materials	Bulk Modulus, MPa	Density, kg/m ³
Structural steel (Steel ball)	25	7850
CONC-30MPA (Plain concrete)	30	2314

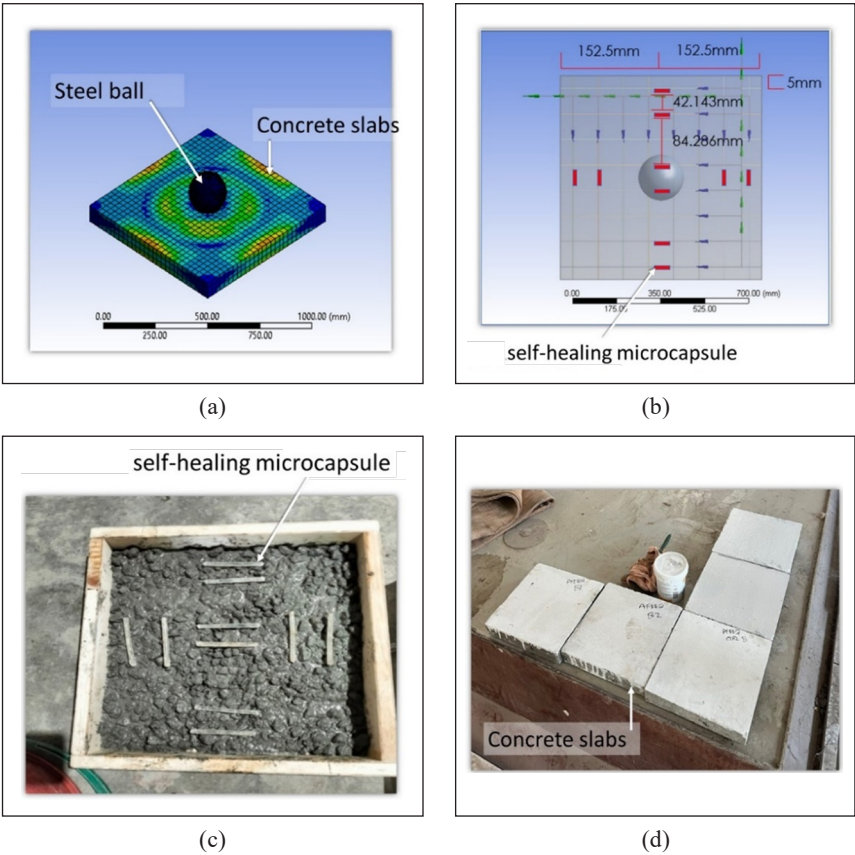


Figure 3. (a) The explicit dynamic analysis on the concrete slab model; (b) Schematic diagram of the microcapsule position; (c) Experimental arrangement layouts of self-healing microcapsules inside concrete slab specimens; and (d) Concrete slab specimens with white bottom surfaces

between each two microcapsules at the centre and each side of the specimens was 42.14 mm, excluding the 5mm concrete covers as seen in Figure 3(c). The distance between each segment location of self-healing microcapsules was 84.29 mm.

Mix Proportion Design of Concrete Slabs

The specimens of concrete slabs were prepared at the laboratory of the University Tenaga Nasional. The size of the concrete slab specimens prepared for the impact test is 305 mm × 305 mm × 50 mm, with specific arrangements of self-healing microcapsules. The mix proportion ofw the specimens was determined through the measurements in the Department of Environment (DOE) method and according to the BS 8500 standards (Azman et al., 2023; Jang et al., 2017). The mix ratio of the specimens is 1:1.7:2.9, which is designed to surpass the compressive strength at 30 MPa. The water/cement ratio of the concrete slab is 0.4. The weight of each material used to prepare a concrete slab is presented in Table 3. The curing condition for the prepared specimens is inside plain water at ambient temperature.

Table 3
Mix proportion of concrete slab specimens

OPC, kg	Fine Agg., kg	Coarse Agg., kg	Water, kg
1.86	3.14	5.42	0.82

Eight concrete slab specimens were cast, consisting of two controlled specimens (LC and SC), one large self-healing microcapsule with three repetitions denoted as L1, L2, and L3. On the other hand, one small self-healing microcapsule with three repetitions is denoted as S1, S2 and S3. The materials used are ordinary Portland cement (OPC), fine aggregates of sand, coarse aggregates of gravel, and a sufficient amount of water. The fine and coarse aggregates were sieved below 5 mm and between 9 and 12 mm, respectively (Jang et al., 2017).

The slump result achieved from the fresh concrete was 10 mm, which, according to the BS EN 12350–2 standards, proved to be a true slump with good workability (Zheng & Qian, 2020). The fresh concrete was then added into the formwork with a size of 305 mm × 305 mm × 50 mm, in the form of three layers and vibrated using the vibration machine to prevent air voids and specimen bleeding (Amran et al., 2022). A total of ten each for large and small microcapsules were added into the fresh mix at the first layer in an orthogonal arrangement, which replicated the crack pattern of the concrete slab in the simulation. Then, the second and third layers of fresh mix were poured consequently and left to harden for 24 hours. After the specimens were cured for 28 days, it was painted white on the bottom surface for ease of visibility of cracks as seen in Figure 3(d) (Huang & Zhou, 2022).

METHODOLOGY

Compressive Strength

The compressive strength was conducted to show that the formulation of the RC slab used in this study had the minimum compressive strength required according to BS EN 12390-3 standards (Hu et al., 2018). The compressive strength test was performed for all eight concrete cube specimens after 28 days of curing. The sizes of the cube specimens were prepared at 100 mm × 100 mm × 100 mm to surpass the compressive strength of 30 MPa, tested after 28 days of curing. A universal testing machine (UTM) conducted the compressive strength test. The dimensions and weight of the specimens were inserted into the UTM software, and the specimens were labelled. Then, the specimens were placed at the centre of the UTM machine, pushed and compressed with two opposite forces until they reached failure (Hu et al., 2018). Afterwards, the result of compressive strength of the specimens was recorded, as presented in Figure 4.

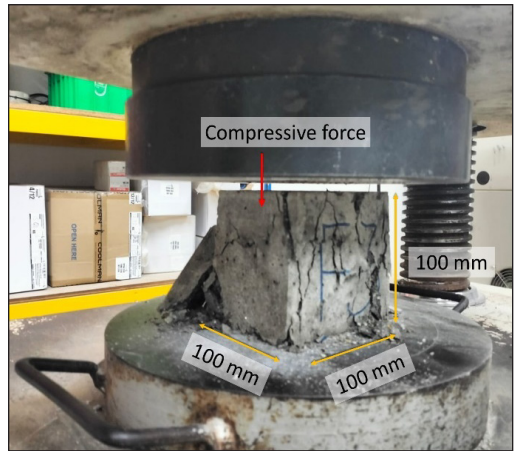


Figure 4. Cube compression test on a concrete cube specimen

Drop Weight

The drop weight test is a low-velocity impact test to measure the impact energy or impact resistance of an RC structure, especially the concrete slab specimens. The test is performed according to the BS EN 1621-1:1998 standards. Initially, 305 mm × 305 mm × 50 mm concrete specimens were placed on a flat stand and clamped at four-sided fixed supports using G-clamps. The stainless-steel ball impactor with a weight of 4 kg and a diameter of 110 mm was placed on top of the steel slide to free fall by gravity to hit the top surface of the concrete slab specimens. The height of the impactor from the top surface of the concrete slab was determined by using the formula of impact energy as presented in Equation 3.

$$E = Nmgh \quad [3]$$

The energy, E , of the impact is obtained through the number of hits of the impactor, N , combined with mass, gravity and height, which are m , g and h , respectively. However, the calculation of the height, h , can be made by exclusion of the number of hits, N , as it is only used to evaluate the initial and ultimate cracks of the specimens while dividing it with the dimension of the specimens at 305 mm × 305 mm × 50 mm to create a correlation

measurement. The height of the impactor from the top surface of the concrete slab was approximately 175.24 mm. Later, the impactor was released once at a time, and the bottom surfaces of the specimens were observed for initial cracking until ultimate cracking occurred. The reduction of cracks in the specimens due to the efficiency rate of the self-healing microcapsules was observed and recorded day-to-day. The setup of the drop weight test is presented in Figure 5. Using a single impact location may not provide a comprehensive understanding of concrete self-healing performance as reflected in the real-life scenario. However, it offers valuable insights into how the concrete self-healing mechanism works when subjected to impact in this specific study.

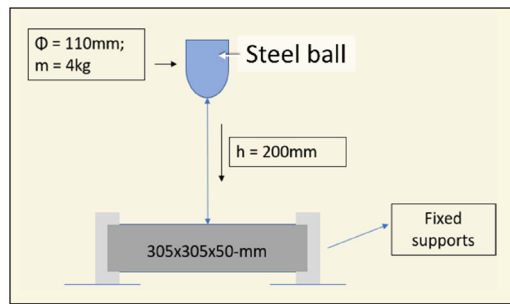
RESULTS AND DISCUSSION

Compressive Strength

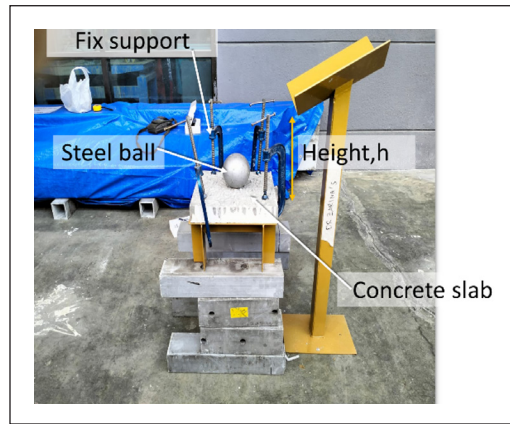
The compressive strength results demonstrated by eight concrete cube specimens were adequate for the industry's concrete structure, as they achieved results within the range of the compressive strength at 30 MPa. The failure patterns of the concrete cube specimens formed prism shapes, which followed the BS EN 12390-3 standards (Hu et al., 2018). Furthermore, the compressive strength obtained from the cube specimens was identical to the strength of the concrete slab specimens, as their fresh concrete mixture was cast together during the experiment (Qureshi & Al-Tabbaa, 2020; Wang et al., 2014). The compressive strength results were 33.68 MPa ($S=5.23$).

Low Velocity Impact of Concrete Slab with Self-Healing Microcapsules

The drop weight test was performed on two controlled concrete slabs, three with large self-healing microcapsules, and three with small self-healing microcapsules according to the BS EN 1621-1:1998 standards. The number of hits, N , from the stainless-steel ball impactor to the top surface of the concrete slab specimens was below twenty hits to obtain the ultimate cracks. Furthermore, the ultimate cracks obtained by eight concrete slab specimens do not exceed 2.5 mm, which is suitable for self-healing agents to seep



(a)



(b)

Figure 5. (a) The schematic; and (b) The setup of the drop weight test

through the gaps and reduce the crack widths (Maddalena et al., 2021). The results of the impact test on the specimens, LC, L1, L2, L3, SC, S1, S2 and S3 are recorded in Tables 4, 5, 6 and 7, respectively.

Based on Tables 3 to 6, there were three points of crack widths on concrete slab specimens parallel to the location of the self-healing microcapsule that were recorded after each hit from the impactor in a weight drop test. The test results demonstrated that the concrete slab specimens with microcapsules can withstand more impact hits compared to the controlled concrete slab specimens. The maximum number of impact hits, N, obtained by the controlled concrete slabs, LC and SC, was nine hits. At the same time, the specimens with large and small self-healing microcapsules, L1, L2, L3 and S1, S2 and S3, received ultimate cracks after 19 hits, 16 hits, 11 hits and 14 hits, 10 hits and 12 hits, respectively. Furthermore, the average crack width displayed by the specimens LC, L1, L2, L3, SC, S1, S2 and S3 was 2.19 mm, 1.21 mm, 1.5 mm, 1.97 mm, 1.99 mm, 1.02 mm, 1.13 mm and 1.28 mm, respectively. The increment and comparison of the number of impacts on the specimens subjected to the drop weight test are presented in Figure 6.

Table 4
The low-velocity impact results of controlled concrete slab LC and L1 with large self-healing microcapsules

Weight drop test	Controlled RC slab, LC			RC slabs with large self-healing microcapsules, L1		
Points No. of Impact, N	Point 1 Crack width, mm	Point 2 Crack width, mm	Point 3 Crack width, mm	Point 1 Crack width, mm	Point 2 Crack width, mm	Point 3 Crack width, mm
1	0	0	0	0	0	0
2	0	0	0	0	0	0
3	0	0	0	0	0	0
4	0	0	0	0	0	0
5	0	0	0	0	0	0
6	0.76	0.53	0.59	0	0	0
7	1.57	0.93	1.34	0	0	0
8	1.88	1.65	1.43	0	0	0
9	2.32	2.08	2.18	0	0	0
10				0	0	0
11				0.16	0.21	0.27
12				0.3	0.5	0.37
13				0.45	0.61	0.53
14				0.62	0.70	0.65
15				0.73	0.72	0.84
16				0.81	0.84	0.87
17				0.92	1.02	0.96
18				1.13	1.10	1.15
19				1.24	1.18	1.20

Table 5
The low-velocity impact results of concrete slabs L2 and L3 with large self-healing microcapsules

Weight drop test	RC slabs with large self-healing microcapsules, L2			RC slabs with large self-healing microcapsules, L3		
Points No. of Impact, N	Point 1 Crack width, mm	Point 2 Crack width, mm	Point 3 Crack width, mm	Point 1 Crack width, mm	Point 2 Crack width, mm	Point 3 Crack width, mm
1	0	0	0	0	0	0
2	0	0	0	0	0	0
3	0	0	0	0	0	0
4	0	0	0	0	0	0
5	0	0	0	0	0	0
6	0	0	0	0	0	0
7	0	0	0	0.18	0.21	0.15
8	0	0	0	0.35	0.41	0.47
9	0	0	0	0.59	0.63	0.62
10	0.23	0.21	0.21	1.78	1.19	1.65
11	0.46	0.44	0.43	2	1.94	1.98
12	0.51	0.55	0.52			
13	0.66	0.70	0.64			
14	0.75	0.75	0.70			
15	1.03	0.97	0.99			
16	1.6	1.4	1.5			

Table 6
The low-velocity impact results of controlled concrete slabs SC and S1 with small self-healing microcapsules

Weight drop test	Controlled RC slab, SC			RC slabs with small self-healing microcapsules, S1		
Points No. of Impact, N	Point 1 Crack width, mm	Point 2 Crack width, mm	Point 3 Crack width, mm	Point 1 Crack width, mm	Point 2 Crack width, mm	Point 3 Crack width, mm
1	0	0	0	0	0	0
2	0	0	0	0	0	0
3	0	0	0	0	0	0
4	0	0	0	0	0	0
5	0.14	0.13	0.17	0	0	0
6	0.36	0.23	0.31	0	0	0
7	0.75	0.71	0.72	0	0	0
8	1.69	1.43	1.6	0	0	0
9	2	2.04	1.93	0	0	0
10				0	0	0
11				0.14	0.09	0.11
12				0.43	0.38	0.42
13				0.76	0.74	0.68
14				1.07	0.97	1.03

Table 7
The low-velocity impact results of concrete slabs S2 and S3 with small self-healing microcapsules

Weight drop test	RC slabs with small self-healing microcapsules, S2			RC slabs with small self-healing microcapsules, S3		
Points	Point 1	Point 2	Point 3	Point 1	Point 2	Point 3
No. of Impact, N	Crack width, mm	Crack width, mm	Crack width, mm	Crack width, mm	Crack width, mm	Crack width, mm
1	0	0	0	0	0	0
2	0	0	0	0	0	0
3	0	0	0	0	0	0
4	0	0	0	0	0	0
5	0	0	0	0	0	0
6	0	0	0	0	0	0
7	0.29	0.23	0.25	0	0	0
8	0.57	0.62	0.6	0.36	0.37	0.32
9	0.75	0.83	0.86	0.6	0.43	0.5
10	1.17	1.09	1.12	0.84	0.79	0.91
11				1.19	1.02	1.14
12				1.32	1.21	1.31

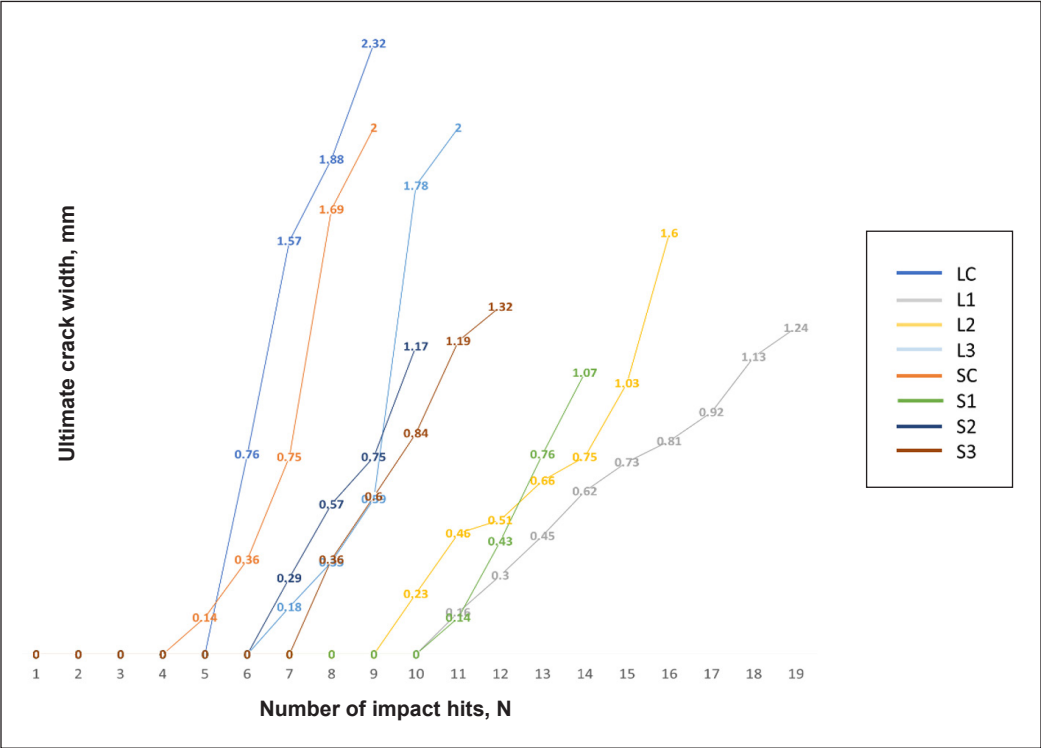


Figure 6. The number of impact hits on the concrete slab specimens

Based on Figure 6, the overall number of impact hits, N , received by the concrete slab specimens were systematic as its maximum hits was below the 50 hits which led to the structure prevented from obtained any severe defects such as spalling or delamination of steel reinforcement bars as according to BS EN 1992-2 standards (Frigo et al., 2017). The impact on specimen L1 was 10 hits more compared to specimen LC. Meanwhile, in terms of the highest number of impacts on the large and small self-healing microcapsules inside concrete slab specimens, the specimen L1 achieved more impact by five hits compared to the specimen S1. Though the specimens were similar in size, curing days and mix design, the hit numbers still varied, resulting from the small air voids or improper distribution of materials in the specimens (Raza et al., 2023).

The Efficiency of Crack Size Reductions on Concrete Slabs with Self-Healing Microcapsules

The ultimate crack widths that occurred on eight concrete slab specimens consisted of two controlled RC slabs, three R concrete slabs with large self-healing microcapsules and three concrete slabs with small self-healing microcapsules were varied in general due to the difference in number of low velocity impact hits, N . Overall, all specimens obtained self-healing process after the self-healing microcapsules that contained sodium silicate liquidation were released resulted from the breaking of the encapsulation from impact (Maddalena et al., 2021; Kahar et al., 2021). All specimens displayed an orthogonal crack pattern of length 152.5 mm from the centre of the specimens. The average reduction in the size of the crack width of specimens is presented in Table 8.

Based on Table 7, there are three main points of ultimate crack on specimens that displayed self-healing process, where the crack was above the location of the large and small self-healing microcapsules. The reduction of cracks at the three points mentioned for the specimens was measured and recorded as an average crack reduction in 28 days. The average crack reductions of specimens LC, L1, L2, L3, SC, S1, S2 and S3 were 2.19 mm, 0.28 mm, 0.36 mm, 0.42 mm, 1.99 mm, 0.99 mm, 1.07 mm and 1.25 mm, respectively. The average crack of specimens, L1, L2, L3, S1, S2 and S3 were reduced by 0.93 mm, 1.14 mm, 1.55 mm, 0.03 mm, 0.06 mm, and 0.03 mm from its original crack width of 1.21 mm, 1.5 mm, 1.97 mm, 1.02 mm, 1.13 mm and 1.28 mm, correspondingly. However, both the ultimate cracks on the controlled concrete slab specimens, LC and SC, have no self-healing process because of the absence of the large and small self-healing microcapsules. The visible crack reductions on the specimens L1, L2, L3, S1, S2, and S3 in 28 days were consistently fast due to the efficiency of the volume of sodium silicate liquidation reaction with the cementitious-based chemical inside the specimens, as presented in Table 9. The healing process is monitored from day one by circling the area of the crack. The circled area of the crack is checked daily, and the width of the crack is recorded using a microscope

Table 8
The size reduction of cracks on concrete slab specimens

Weight drop test		The process of self-healing in days									Crack reduction, mm
Specimens	Points	1	3	5	7	11	14	18	21	28	Average
Controlled, LC	Point 1	2.32	2.32	2.32	2.32	2.32	2.32	2.32	2.32	2.32	2.19
	Point 2	2.08	2.08	2.08	2.08	2.08	2.08	2.08	2.08	2.08	
	Point 3	2.18	2.18	2.18	2.18	2.18	2.18	2.18	2.18	2.18	
L1	Point 1	1.24	0.72	0.59	0.32	0.28	0.28	0.28	0.28	0.28	0.28
	Point 2	1.18	0.8	0.74	0.30	0.28	0.26	0.26	0.26	0.26	
	Point 3	1.20	0.7	0.62	0.36	0.31	0.31	0.31	0.31	0.31	
L2	Point 1	1.6	1.26	0.7	0.61	0.53	0.38	0.38	0.38	0.38	0.36
	Point 2	1.4	1.27	0.4	0.39	0.37	0.36	0.36	0.35	0.35	
	Point 3	1.5	1.19	0.68	0.61	0.43	0.43	0.43	0.38	0.37	
L3	Point 1	2	1.52	0.83	0.58	0.47	0.45	0.45	0.45	0.45	0.42
	Point 2	1.94	0.99	0.82	0.7	0.65	0.53	0.44	0.42	0.42	
	Point 3	1.98	1.65	1.25	1.03	1.03	0.74	0.53	0.41	0.4	
Controlled, SC	Point 1	2	2	2	2	2	2	2	2	2	1.99
	Point 2	2.04	2.04	2.04	2.04	2.04	2.04	2.04	2.04	2.04	
	Point 3	1.93	1.93	1.93	1.93	1.93	1.93	1.93	1.93	1.93	
S1	Point 1	1.07	1.07	1.05	1.05	1.04	1.04	1.04	1.04	1.04	0.99
	Point 2	0.97	0.96	0.95	0.95	0.95	0.94	0.94	0.94	0.94	
	Point 3	1.03	1.02	1.02	1	1	1	1	1	1	
S2	Point 1	1.17	1.15	1.15	1.14	1.14	1.14	1.14	1.14	1.14	1.07
	Point 2	1.09	1.07	1.07	1.07	1.07	1.06	1.06	1.06	1.06	
	Point 3	1.12	1.1	1.1	1.1	1.09	1.09	1.09	1.09	1.09	
S3	Point 1	1.32	1.32	1.3	1.3	1.3	1.3	1.3	1.3	1.3	1.25
	Point 2	1.21	1.20	1.19	1.17	1.17	1.17	1.17	1.17	1.17	
	Point 3	1.31	1.30	1.29	1.29	1.29	1.29	1.28	1.28	1.28	

at the laboratory. The width of the crack reduction from day one until the end of the 28th day is recorded.

Based on Table 8, all specimens besides the controlled specimens, LC and SC, obtained self-healing effectively and reduced the original ultimate cracks up to a certain width. The efficiency in the healing process was increased by 87.2%, 83.6% and 80.8% for the Specimens L1, L2 and L3 with the large self-healing microcapsules compared to their controlled specimens. Moreover, in comparison to the controlled specimen, the specimens S1, S2, and S3 with the small self-healing microcapsules displayed an increment in healing efficiency of 50.3%, 46.2%, and 37.2%, respectively. Hence, the efficiency difference between the specimens with large self-healing microcapsules and small self-healing microcapsules was 68.2%, where the large microcapsules contributed more to the self-healing of specimens compared to the small microcapsules.

Table 9
Concrete slab specimens with large and small self-healing microcapsules before and after the 28-day self-healing process







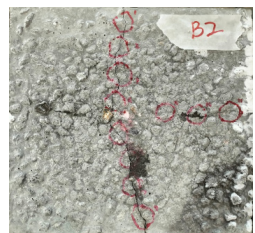

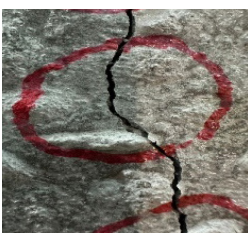




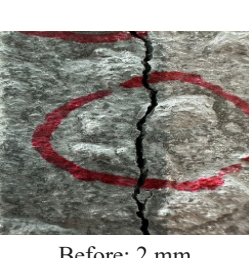

Specimens	Point 1	Point 2	Point 3
Specimen L1			
	Before: 1.24 mm	Before: 1.18 mm	Before: 1.20 mm
			
	After: 0.28 mm	After: 0.26 mm	After: 0.31 mm
Specimen L2			
	Before: 1.6 mm	Before: 1.4 mm	Before: 1.5 mm
			
	After: 0.38 mm	After: 0.35 mm	After: 0.37 mm
Specimen L3			
	Before: 2 mm	Before: 1.94mm	Before: 1.98 mm

Table 9 (continue)





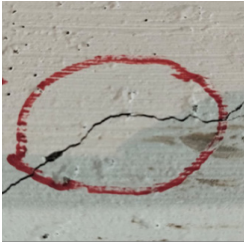





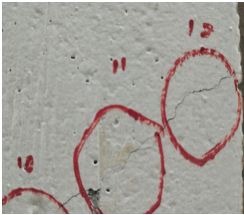

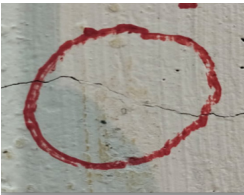
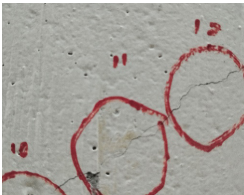
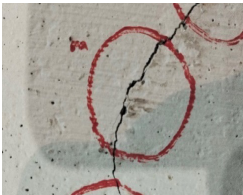
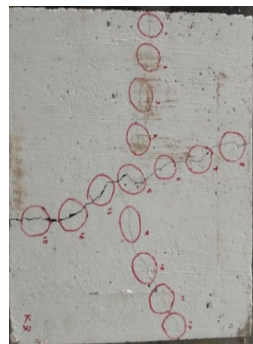

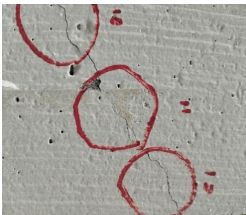
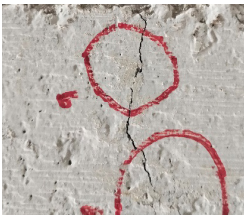
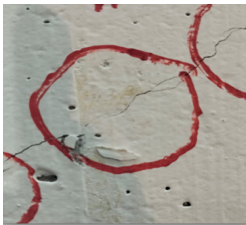
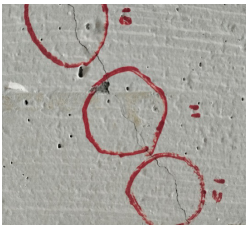

Specimens	Point 1	Point 2	Point 3
	 After: 0.45 mm	 After: 0.42 mm	 After: 0.4 mm
Specimen S1	 Before: 1.07 mm	 Before: 0.97 mm	 Before: 1.03 mm
	 After: 1.04 mm	 After: 0.94 mm	 After: 1 mm
Specimen S2	 Before: 1.17 mm	 Before: 1.09 mm	 Before: 1.12 mm
	 After: 1.14 mm	 After: 1.06 mm	 After: 1.09 mm

Table 9 (continue)

Specimens	Point 1	Point 2	Point 3
 Specimen S3	 Before: 1.32 mm	 Before: 1.21 mm	 Before: 1.31 mm
	 After: 1.3 mm	 After: 1.17 mm	 After: 1.28 mm

The crack widths dominant at specimens L1, L2 and L3, demonstrated that the larger size of the self-healing microcapsules resulted in the RC slab becoming slightly fragile due to the volume of PLA and PMMA materials consuming space in the specimens, with their low tensile break points (Ridwan et al., 2017). However, the sodium silicate liquidation inside the self-healing microcapsules compromised the strength loss and managed to repair the cracks from inside to outside of the ultimate cracks on the specimens, as the volume and spread radius of the liquidation were within the critical zones of the specimens (Sabee et al., 2022). Furthermore, the process of self-healing in specimens S1, S2 and S3 was slow and less so due to the volume of sodium silicate liquidation in the small self-healing microcapsules, which can only occupy a small range of crack gaps from their encapsulation sources (Muda et al., 2016; Kahar et al., 2021).

CONCLUSION

The research on the efficiency of the self-healing microcapsules in concrete slab specimens subjected to low velocity impact force was successful in 28 days. The maximum number of impact hits, N, obtained by the controlled concrete slabs, LC and SC, was nine hits. At the same time, the specimens with large and small self-healing microcapsules, L1, L2, L3 and S1, S2 and S3, received ultimate cracks after 19 hits, 16 hits, 11 hits and 14 hits,

10 hits and 12 hits, respectively. The highest and lowest impact hits for specimens with self-healing microcapsules were obtained by specimens L1 and S2, with 19 hits and 10 hits, respectively. Furthermore, the average crack width displayed by the specimens LC, L1, L2, L3, SC, S1, S2 and S3 was 2.19 mm, 1.21 mm, 1.5 mm, 1.97 mm, 1.99 mm, 1.02 mm, 1.13 mm and 1.28 mm, respectively. The results demonstrated that the concrete slab specimens with microcapsules can endure more impact hits compared to the controlled concrete slab specimens. Though the specimens were similar in size, curing days and mix design, the hit numbers still varied, resulting from the small air voids or improper distribution of materials in the specimens.

In terms of the reduction of crack width, the average crack of specimens, L1, L2, L3, S1, S2 and S3 were reduced by 0.93 mm, 1.14 mm, 1.55 mm, 0.03 mm, 0.06 mm and 0.03 mm from its original crack width of 1.21 mm, 1.5 mm, 1.97 mm, 1.02 mm, 1.13 mm and 1.28 mm, correspondingly. Moreover, the ultimate cracks of eight concrete slab specimens do not exceed 2.5 mm, which is suitable for self-healing agents, such as sodium silicate liquidation, to seep through the crack gaps and reduce their width. The efficiency in the healing process was increased by 87.2%, 83.6% and 80.8% for specimens L1, L2, and L3 with the large self-healing microcapsules compared to their controlled specimens. In comparison to the controlled specimen, the specimens S1, S2, and S3 with the small self-healing microcapsules displayed an increment in healing efficiency of 50.3%, 46.2%, and 37.2%, respectively. As a whole, the materials of PLA and PMMA with low tensile properties to break point dominated the concrete slab specimens' volume, thus leading to the crack widths on specimens like specimen LC to be larger than the ultimate crack. The larger size of the self-healing microcapsules led to a slight fragility in specimens. Nevertheless, self-healing microcapsules containing sodium silicate liquidation dealt with the strength loss and repaired the overall ultimate cracks on the specimens.

FUTURE RESEARCH DIRECTION

The future research direction of the work could explore the development of a hybrid triggering mechanism (e.g., mechanical/thermal) of self-healing concrete subjected to high-velocity impact. Besides that, looking into the performance of recycled/reused concrete material promotes sustainable construction practices (Ahmad & Shokouhian, 2024; Akor et al., 2023; Gao, 2023). Machine learning models (e.g., gene expression programming) can help broaden the parameters of the investigation, reducing the cost and time of the investigation and resulting in better data accuracy (Inqiad et al., 2023).

ACKNOWLEDGEMENT

The authors express gratitude to the Innovation & Research Management Centre of Universiti Tenaga Nasional for supporting this research through Project No: BOLD 2022

J510050002/2022024, facilities support from Universiti Sains Malaysia, UNITEN Civil Engineering Laboratory, J510050002/HICOE05 for the journal publication fees and BOLD Refresh Postdoctoral Fellowships under Grant J510050002-IC-6 BOLDREFRESH2025-Centre of Excellence.

REFERENCES

- Ahmad, I., & Shokouhian, M. (2024). Promoting sustainable green infrastructure: Experimental and numerical investigation of concrete reinforced with recycled steel fibers. *Archives of Advanced Engineering Science*, 3(1), 1-13. <https://doi.org/10.47852/bonviewAAES42022837>
- Akor, J., Onjefu, L., Edeh, J., & Olubambi, A. (2023). Suitability of crushed sandcrete block (CSB) as a partial replacement for fine aggregate in concrete structures. *Archives of Advanced Engineering Science*, 3(1), 1-9. <https://doi.org/10.47852/bonviewAAES32021741>
- Althoe, F., Zaid, O., Arbili, M. M., Martínez-García, R., Alhamami, A., Shah, H. A., & Yosri, A. M. (2023). Physical, strength, durability and microstructural analysis of self-healing concrete: A systematic review. *Case Studies in Construction Materials*, 18, Article e01730. <https://doi.org/10.1016/j.cscm.2022.e01730>
- Amran, M., Onaizi, A. M., Fediuk, R., Vatin, N. I., Rashid, R. S. M., Abdelgader, H., & Ozbakkaloglu, T. (2022). Self-healing concrete as a prospective construction material: A review. *Materials*, 15(9), Article 3214. <https://doi.org/10.3390/ma15093214>
- Azman, N. A., Syamsir, A., Bakar, M. S. A., Rizal, M. A. M., Sanusi, K. A., & Abdullah, M. J. (2023). The characteristics of polymer concrete reinforced with polypropylene fibres under axial and lateral compression loads. *Pertanika Journal of Science and Technology*, 31(3), 1535 - 1554. <https://doi.org/10.47836/pjst.31.3.23>
- Dixit, A. C., Achutha, M. V., & Sridhara, B. K. (2021). Elastic properties of aluminum boron carbide metal matrix composites. *Materials Today: Proceedings*, 43, 1253–1257. <https://doi.org/10.1016/j.matpr.2020.08.766>
- Durga, C. S. S., Ruben, N., Chand, M. S. R., Indira, M., & Venkatesh, C. (2021). Comprehensive microbiological studies on screening bacteria for self-healing concrete. *Materialia*, 15, Article 101051. <https://doi.org/10.1016/j.mtla.2021.101051>
- Ferrara, L., Van Mullem, T., Alonso, M. C., Antonaci, P., Borg, R. P., Cuenca, E., Jefferson, A., Ng, P. L., Peled, A., Roig-Flores, M., Sanchez, M., Schroefl, C., Serna, P., Snoeck, D., Tulliani, J. M., & De Belie, N. (2018). Experimental characterization of the self-healing capacity of cement-based materials and its effects on the material performance: A state of the art report by COST Action SARCOS WG2. *Construction and Building Materials*, 167, 115–142. <https://doi.org/10.1016/j.conbuildmat.2018.01.143>
- Frigo, B., Fantilli, A. P., & Chiaia, B. (2017). Size effect on fracture toughness of snow. *Procedia Structural Integrity*, 3, 261–268. <https://doi.org/10.1016/j.prostr.2017.04.028>
- Gao, J., Jin, P., Zhang, Y., Dong, H., & Wang, R. (2022). Fast-responsive capsule based on two soluble components for self-healing concrete. *Cement and Concrete Composites*, 133, Article 104711. <https://doi.org/10.1016/j.cemconcomp.2022.104711>

- Gao, X. (2023). Review: Development trends in the reuse of waste materials in concrete production. *Academic Journal of Science and Technology*, 8(2), 26–30. <https://doi.org/10.54097/ajst.v8i2.14714>
- Gupta, S., Pang, S. D., & Kua, H. W. (2017). Autonomous healing in concrete by bio-based healing agents – A review. *Construction and Building Materials*, 146, 419–428. <https://doi.org/10.1016/j.conbuildmat.2017.04.111>
- Hilloulin, B., Van Tittelboom, K., Gruyaert, E., De Belie, N., & Loukili, A. (2015). Design of polymeric capsules for self-healing concrete. *Cement and Concrete Composites*, 55, 298–307. <https://doi.org/10.1016/j.cemconcomp.2014.09.022>
- Homma, D., Mihashi, H., & Nishiwaki, T. (2009). Self-healing capability of fibre reinforced cementitious composites. *Journal of Advanced Concrete Technology*, 7(2), 217–228. <https://doi.org/10.3151/jact.7.217>
- Hu, Z. X., Hu, X. M., Cheng, W. M., Zhao, Y. Y., & Wu, M. Y. (2018). Performance optimization of one-component polyurethane healing agent for self-healing concrete. *Construction and Building Materials*, 179, 151–159. <https://doi.org/10.1016/j.conbuildmat.2018.05.199>
- Huang, F., & Zhou, S. (2022). A review of lightweight self-healing concrete. *Materials*, 15(21), Article 7572. <https://doi.org/10.3390/ma15217572>
- Inqiad, W., Raza, M. A., & Asim, M. (2023). Predicting 28-day compressive strength of self-compacting concrete (SCC) using gene expression programming (GEP). *Archives of Advanced Engineering Science*, 3(1), 1-13. <https://doi.org/10.47852/bonviewAAES32021606>
- Irico, S., Bovio, A. G., Paul, G., Boccaleri, E., Gastaldi, D., Marchese, L., Buzzi, L., & Canonico, F. (2017). A solid-state NMR and X-ray powder diffraction investigation of the binding mechanism for self-healing cementitious materials design: The assessment of the reactivity of sodium silicate based systems. *Cement and Concrete Composites*, 76, 57–63. <https://doi.org/10.1016/j.cemconcomp.2016.11.006>
- Jakubovskis, R., Jankutė, A., Urbonavičius, J., & Gribniak, V. (2020). Analysis of mechanical performance and durability of self-healing biological concrete. *Construction and Building Materials*, 260, Article 119822. <https://doi.org/10.1016/j.conbuildmat.2020.119822>
- Jang, H. O., Lee, H. S., Cho, K., & Kim, J. (2017). Experimental study on shear performance of plain construction joints integrated with ultra-high performance concrete (UHPC). *Construction and Building Materials*, 152, 16–23. <https://doi.org/10.1016/j.conbuildmat.2017.06.156>
- Jogi, P. K., & Lakshmi, T. V. S. V. (2021). Self healing concrete based on different bacteria: A review. *Materials Today: Proceedings*, 43, 1246–1252. <https://doi.org/10.1016/j.matpr.2020.08.765>
- Kahar, N. N. F. N. M. N., Osman, A. F., Alosime, E., Arsath, N., Azman, N. A. M., Syamsir, A., Itam, Z., & Hamid, Z. A. A. (2021). The versatility of polymeric materials as self-healing agents for various types of applications: A review. *Polymers*, 13(8), Article 1194. <https://doi.org/10.3390/polym13081194>
- Khaliq, W., & Ehsan, M. B. (2016). Crack healing in concrete using various bio influenced self-healing techniques. *Construction and Building Materials*, 102, 349–357. <https://doi.org/10.1016/j.conbuildmat.2015.11.006>
- Li, J., & Guan, X. (2023). Pretreated lightweight aggregates for self-healing concrete exposed to calcium hydroxide-rich sewage. *Construction and Building Materials*, 365, Article 130117. <https://doi.org/10.1016/j.conbuildmat.2022.130117>

- Lv, L., Guo, P., Liu, G., Han, N., & Xing, F. (2020). Light induced self-healing in concrete using novel cementitious capsules containing UV curable adhesive. *Cement and Concrete Composites*, 105, Article 103445. <https://doi.org/10.1016/j.cemconcomp.2019.103445>
- Lv, Z., Yao, J., Cui, G., & Chen, H. (2022). Geometrical probability of a capsule hitting irregular crack networks: Application to capsule-based self-healing materials. *Applied Mathematical Modelling*, 101, 406–419. <https://doi.org/10.1016/j.apm.2021.08.031>
- Maddalena, R., Taha, H., & Gardner, D. (2021). Self-healing potential of supplementary cementitious materials in cement mortars: Sorptivity and pore structure. *Developments in the Built Environment*, 6, Article 100044. <https://doi.org/10.1016/j.dibe.2021.100044>
- Mir, N., Khan, S. A., Kul, A., Sahin, O., Ozcelikci, E., Sahmaran, M., & Koc, M. (2023). Construction and demolition waste-based self-healing geopolymer composites for the built environment: An environmental profile assessment and optimization. *Construction and Building Materials*, 369, Article 130520. <https://doi.org/10.1016/j.conbuildmat.2023.130520>
- Mokhtar, N., & Hassan, M. F. M. (2021). Performance of sodium silicate as self-healing agent on concrete properties: A review. *IOP Conference Series: Materials Science and Engineering*, 1144(1), Article 012024. <https://doi.org/10.1088/1757-899X/1144/1/012024>
- Muda, Z. C., Kamal, N. L. M., Syamsir, A., Sheng, C. Y., Beddu, S., Mustapha, K. N., Thiruchelvam, S., Usman, F., Alam, M. A., Birima, A. H., & Zaroog, O. S. (2016). Impact resistance performance of kenaf fibre reinforced concrete. *IOP Conference Series: Earth and Environmental Science*, 32, Article 012019. <https://doi.org/10.1088/1755-1315/32/1/012019>
- Muhammad, N. Z., Shafaghat, A., Keyvanfar, A., Majid, M. Z. A., Ghoshal, S. K., Yasouj, S. E. M., Ganiyu, A. A., Kouchaksaraei, M. S., Kamyab, H., Taheri, M. M., Shirdar, M. R., & McCaffer, R. (2016). Tests and methods of evaluating the self-healing efficiency of concrete: A review. *Construction and Building Materials*, 112, 1123–1132. <https://doi.org/10.1016/j.conbuildmat.2016.03.017>
- Qureshi, T., & Al-Tabbaa, A. (2020). Self-healing concrete and cementitious materials. In N. Tasaltin, P. S. Nnamchi & S. Saud (Eds.), *Advanced Functional Materials* (pp. 191–214). IntechOpen. <https://doi.org/10.5772/intechopen.92349>
- Raza, A., El Ouni, M. H., uz Zaman Khan, Q., Azab, M., Khan, D., Elhadi, K. M., & Alashker, Y. (2023). Sustainability assessment, structural performance and challenges of self-healing bio-mineralized concrete: A systematic review for built environment applications. *Journal of Building Engineering*, 66, Article 105839. <https://doi.org/10.1016/j.jobe.2023.105839>
- Ren, J., Wang, X., Li, D., Han, N., Dong, B., & Xing, F. (2021). Temperature adaptive microcapsules for self-healing cementitious materials. *Composites Part B: Engineering*, 223, Article 109138. <https://doi.org/10.1016/j.compositesb.2021.109138>
- Restuccia, L., Reggio, A., Ferro, G. A., & Tulliani, J. M. (2017). New self-healing techniques for cement-based materials. *Procedia Structural Integrity*, 3, 253–260. <https://doi.org/10.1016/j.prostr.2017.04.016>
- Ridwan, M., Yoshitake, I., & Nassif, A. Y. (2017). Two-dimensional fictitious truss method for estimation of out-of-plane strength of masonry walls. *Construction and Building Materials*, 152, 24–38. <https://doi.org/10.1016/j.conbuildmat.2017.06.138>

- Rosewitz, J. A., Wang, S., Scarlata, S. F., & Rahbar, N. (2021). An enzymatic self-healing cementitious material. *Applied Materials Today*, 23, Article 101035. <https://doi.org/10.1016/j.apmt.2021.101035>
- Sabee, M. M. S. M., Itam, Z., Beddu, S., Zahari, N. M., Kamal, N. L. M., Mohamad, D., Zulkepli, N. A., Shafiq, M. D., & Hamid, Z. A. A. (2022). Flame retardant coatings: Additives, binders, and fillers. *Polymers*, 14(14), Article 2911. <https://doi.org/10.3390/polym14142911>
- Van Tittelboom, K., De Belie, N., Van Loo, D., & Jacobs, P. (2011). Self-healing efficiency of cementitious materials containing tubular capsules filled with healing agent. *Cement and Concrete Composites*, 33(4), 497–505. <https://doi.org/10.1016/j.cemconcomp.2011.01.004>
- Vijay, K., Murmu, M., & Deo, S. V. (2017). Bacteria based self healing concrete – A review. *Construction and Building Materials*, 152, 1008–1014. <https://doi.org/10.1016/j.conbuildmat.2017.07.040>
- Wang, J. Y., Soens, H., Verstraete, W., & De Belie, N. (2014). Self-healing concrete by use of microencapsulated bacterial spores. *Cement and Concrete Research*, 56, 139–152. <https://doi.org/10.1016/j.cemconres.2013.11.009>
- Xiong, W., Tang, J., Zhu, G., Han, N., Schlangen, E., Dong, B., Wang, X., & Xing, F. (2015). A novel capsule-based self-recovery system with a chloride ion trigger. *Scientific Reports*, 5(1), Article 10866. <https://doi.org/10.1038/srep10866>
- Yıldırım, G., Şahmaran, M., & Anıl, Ö. (2018). Engineered cementitious composites-based concrete. In F. Pacheco-Torgal, R. E. Melchers, X. Shi, N. De Belie, K. Van Tittelboom & A. Sáez (Eds.), *Eco-Efficient Repair and Rehabilitation of Concrete Infrastructures* (pp. 387–427). Elsevier. <https://doi.org/10.1016/B978-0-08-102181-1.00015-0>
- Zhang, W., Zheng, Q., Ashour, A., & Han, B. (2020). Self-healing cement concrete composites for resilient infrastructures: A review. *Composites Part B: Engineering*, 189, Article 107892. <https://doi.org/10.1016/j.compositesb.2020.107892>
- Zheng, T., & Qian, C. (2020). Influencing factors and formation mechanism of CaCO₃ precipitation induced by microbial carbonic anhydrase. *Process Biochemistry*, 91, 271–281. <https://doi.org/10.1016/j.procbio.2019.12.018>